Polyhedron 92 (2015) 37–40

Contents lists available at ScienceDirect

Polyhedron

journal homepage: www.elsevier.com/locate/poly

Binding of a Dy(III) complex to apoferritin inhibits iron mineralization

Zichen Xu [a,c], Lei Zhang [a,*], Dongmei Li [b,*], Xiyun Liu [a], Yuxia Wang [c], Jianping Lin [b]

[a] Institute of Modern Optics and MOE Key Laboratory of Optical Information Science & Technology, Nankai University, Tianjin 300071, PR China
[b] College of Pharmacy, Nankai University, Tianjin 300071, PR China
[c] College of Chemistry, Nankai University, Tianjin 300071, PR China

ARTICLE INFO

Article history:
Received 13 January 2015
Accepted 11 March 2015
Available online 21 March 2015

Keywords:
Rare earth
Apoferritin
Bioinorganic chemistry
Nanocomposite
Iron mineralization

ABSTRACT

Apoferritin is a versatile platform for encapsulating a variety of materials, such as inorganic particles and metal complexes, in its nanocavity. However, loading apoferritin with rare earth metal complexes has been less studied, let alone investigating the binding effect of rare earth metal complexes on iron mineralization in apoferritin. In this work, a new cationic Dy(III) complex, $[Dy(NO_3)(H_2O)(tmp)_2](NO_3)_2$ (tmp = trimethylolpropane), was synthesized and subsequently loaded in apoferritin. The binding of the Dy(III) complex to apoferritin inhibited iron mineralization, a plausible explanation being that the early recognition of Fe^{2+} at the ferroxidase sites was disrupted as a result of the binding of the Dy(III) complex.

1. Introduction

Ferritin, best known as an iron-storage protein, has received constant research attention in biological inorganic chemistry on the basis of its intriguing structure and function [1–4]. The protein component, apoferritin, is composed of 24 subunits that assemble as a hollow rhombic dodecahedral protein shell with an outer diameter of about 12 nm and an internal cavity diameter of the order of 8 nm [5]. The junctions of these subunits provide eight 3-fold and six 4-fold channels that perforate the protein shell and serve as pathways between the exterior and interior [6,7]. For basic research on the structure–function relationship, a recent study revealed the involvement of both 3-fold and 4-fold channels in diffusing Fe^{2+} into the cavity of plant ferritin [8]. The possible association between serum ferritin and cancer, as well as the application of ferritin-based materials in cancer theranostics, has also attracted interdisciplinary research interest [9–11]. It is noteworthy that in a novel work, magnetoferritin nanoparticles successfully bound to tumor cells that overexpressed transferrin receptor 1, while the iron oxide nanoparticle core in ferritin was capable of catalyzing an oxidation reaction in the presence of H_2O_2 to produce a color reaction, permitting tumor visualization [12].

One particular area of interest in ferritin research is to take advantage of the confined space provided by ferritin to construct nanocomposite materials. For example, ferritin has been actively explored as a model system to develop new organic/inorganic hybrid photo-catalysts for solar energy harvesting [13]. In these studies, the guest species are mostly inorganic nanoparticles, while a related but different research effort is devoted to loading apoferritin with various metal complexes, such as Pd(allyl) (allyl = η^3-C_3H_5) [14], Ru(II)(η^6-*p*-cymene) (*p*-cymene = 1-methyl-4-(1-methyletheyl)benzene) [15] and Rh(nbd) (nbd = norbornadiene) [16]. The metals in these metal complexes are generally transition metals, but there is an increasing demand to research on the binding of rare earth metal complexes to apoferritin, especially regarding the biomedical implications of these investigations. Moreover, the binding effect of rare earth metal complexes on iron mineralization in apoferritin is an issue that needs to be promptly addressed. In this work, we report the synthesis of a new cationic Dy(III) complex, $[Dy(NO_3)(H_2O)(tmp)_2](NO_3)_2$ (**1**, tmp = trimethylolpropane), its binding to apoferritin, and a property investigation of this nanocomposite system.

2. Experimental

2.1. Materials and methods

All the chemicals used in this work were of analytical reagent grade and used without further purification, unless otherwise stated. Horse spleen apoferritin (HSAF), commercially available from Sigma, was used. 3-(*N*-Morpholino)propanesulfonic acid (MOPS) was purchased from MP Biomedicals. All experiments were

* Corresponding authors. Tel./fax: +86 22 23501242.
E-mail addresses: lzzhang@nankai.edu.cn (L. Zhang), dongmeili@nankai.edu.cn (D. Li).

http://dx.doi.org/10.1016/j.poly.2015.03.009
0277-5387/

performed in 50 mM MOPS, 50 mM NaCl, pH 7.0, unless otherwise specified.

The elemental analysis for C, H and N was carried out on a Perkin–Elmer 240C elemental analyzer. Far-UV circular dichroism measurements were performed on a JASCO J-715 circular dichroism spectrometer at 25 °C. Experimental conditions: scan rate: 20 nm/min; data interval: 1.0 nm; protein concentration: 0.2 mg/mL. Tryptophan fluorescence was measured at 25 °C with an Hitachi F-4500 FL spectrophotometer. Experimental conditions: excitation wavelength: 280 nm; scan rate: 600 nm/min; data interval: 0.2 nm; protein concentration: 0.2 mg/mL.

To determine the number of **1** bound to each HSAF, samples were digested in a 1:1 volume of concentrated HNO_3 at 80 °C for 1 h, followed by analysis with inductively coupled plasma-optical emission spectroscopy (ICP-OES) to determine the Dy concentration. The protein concentration was determined by UV–Vis spectroscopy using the Bradford assay [17].

2.2. Sample preparation

To synthesize **1**, a mixture of $Dy(NO_3)_3$ (34.9 mg, 0.1 mmol), tmp (26.8 mg, 0.2 mmol), and water (10 mL) was sealed in a 25 mL Teflon-lined stainless steel autoclave and heated at 120 °C for 3 days. After cooling to room temperature at a rate of 1.5 °C h^{-1}, white crystals of **1** suitable for structural determination were obtained (yield: 62% based on Dy). *Anal.* Calc. for $C_{12}H_{30}DyN_3O_{16}$: C, 22.70; H, 4.76; N, 6.62. Found: C, 22.50; H, 4.80; N, 6.57%.

To prepare the HSAF–**1** complex, HSAF (20 μM, 250 μL) was mixed with **1** (10 mM, 12 μL) in a **1**:HSAF ratio of 24:1. The reaction mixture was incubated overnight at room temperature, then the samples were dialyzed to remove unbound **1**. Scheme 1 illustrates the procedure for preparing the HSAF–**1** complex.

2.3. X-ray crystallography

The X-ray diffraction data of a single crystal of **1** were collected at 293 ± 2 K on an Oxford diffractometer SuperNova TM with graphite-monochromated Mo Kα radiation (λ = 0.71073 Å) using the ω-scan technique. The structure was solved by direct methods and refined by the full-matrix least-squares technique on F^2 with anisotropic displacement parameters for non-H atoms using the SHELXS-97 and SHELXL-97 programs [18,19]. The hydrogen atoms were placed in idealized positions and constrained to ride on their parent atoms. A summary of the key crystallographic information is given in Table 1. Selected bond lengths and angles are given in Table 2.

Table 1
Crystal data and structure refinement for **1**.

Empirical formula	$C_{12}H_{30}DyN_3O_{16}$
Formula weight	634.89
Crystal system	monoclinic
Space group	$P2_1/c$
a (Å)	9.1801(2)
b (Å)	12.8116(2)
c (Å)	19.7487(4)
α (°)	90.00
β (°)	101.598(2)
γ (°)	90.00
V (Å^3)	2275.26(8)
Z	4
D_{calc} (g cm^{-3})	1.853
$F(000)$	1268
μ (mm^{-1})	3.364
θ range for collection (°)	2.64–25.01
Index ranges	$-10 \leqslant h \leqslant 10$ $-15 \leqslant k \leqslant 14$ $-16 \leqslant l \leqslant 23$
No. of reflections collected	8211
No. of unique reflections	4009
R_{int}	0.0451
No. of observed reflections [$I > 2\sigma(I)$]	2984
Parameters	315
R_1 [$I > 2\sigma(I)$]	0.0348
wR_2 [$I > 2\sigma(I)$]	0.0696
R_1 (all data)	0.0561
wR_2 (all data)	0.0746
GOF	0.966

Table 2
Selected bond lengths (Å) and angles (°) for **1**.

Dy1–O1	2.344(4)	Dy1–O6	2.403(3)
Dy1–O2	2.354(3)	Dy1–O7	2.364(3)
Dy1–O3	2.398(3)	Dy1–O8	2.468(4)
Dy1–O4	2.364(4)	Dy1–O9	2.453(4)
Dy1–O5	2.432(4)		
O1–Dy1–O2	72.53(13)	O3–Dy1–O7	141.31(12)
O1–Dy1–O3	70.85(13)	O3–Dy1–O8	110.29(14)
O1–Dy1–O4	93.61(14)	O3–Dy1–O9	70.68(13)
O1–Dy1–O5	70.07(12)	O4–Dy1–O5	71.74(13)
O1–Dy1–O6	138.30(13)	O4–Dy1–O6	72.27(12)
O1–Dy1–O7	83.50(14)	O4–Dy1–O7	140.65(13)
O1–Dy1–O8	142.02(13)	O4–Dy1–O8	123.38(13)
O1–Dy1–O9	141.09(12)	O4–Dy1–O9	79.49(13)
O2–Dy1–O3	69.45(12)	O5–Dy1–O6	68.25(13)
O2–Dy1–O4	140.76(12)	O5–Dy1–O7	70.43(14)
O2–Dy1–O5	131.40(13)	O5–Dy1–O8	125.93(12)
O2–Dy1–O6	140.83(13)	O5–Dy1–O9	139.41(12)
O2–Dy1–O7	75.57(12)	O6–Dy1–O7	84.02(13)
O2–Dy1–O8	72.82(12)	O6–Dy1–O8	69.39(12)
O2–Dy1–O9	88.78(13)	O6–Dy1–O9	76.16(13)
O3–Dy1–O4	71.33(12)	O7–Dy1–O8	73.24(14)
O3–Dy1–O5	123.17(14)	O7–Dy1–O9	125.30(14)
O3–Dy1–O6	134.17(13)	O8–Dy1–O9	52.09(12)

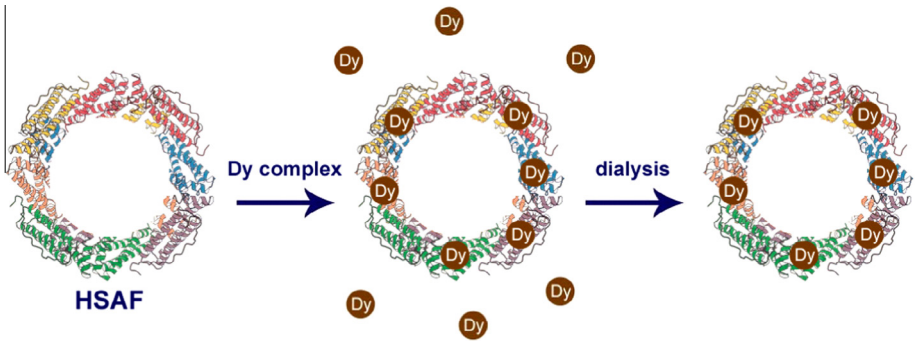

Scheme 1. Schematic illustration of the preparation of the HSAF–**1** complex.